

Deep-ultraviolet Al_{0.75}Ga_{0.25}N photodiodes with low cutoff wavelength

Serkan Butun,^{a)} Turgut Tut, Bayram Butun, Mutlu Gokkavas,
HongBo Yu, and Ekmel Ozbay

Nanotechnology Research Center, Bilkent University, Bilkent, Ankara 06800, Turkey

(Received 27 October 2005; accepted 2 February 2006; published online 21 March 2006)

Deep ultraviolet Al_{0.75}Ga_{0.25}N metal-semiconductor-metal photodetectors with high Al concentration have been demonstrated. A metal-organic chemical vapor deposition grown high quality Al_{0.75}Ga_{0.25}N layer was used as a template. Spectral responsivity, current-voltage, optical transmission, and noise measurements were carried out. The photodetectors exhibited a 229 nm cutoff wavelength and a peak responsivity of 0.53 A/W at 222 nm. Some 100 × 100 μm² devices have shown a dark current density of 5.79 × 10⁻¹⁰ A/cm² under 50 V bias. An ultraviolet-visible rejection ratio of seven orders of magnitude was obtained from the fabricated devices. © 2006 American Institute of Physics. [DOI: 10.1063/1.2186974]

Developments in the past decade have shown that Al_xGa_{1-x}N based materials are suitable especially for detecting ultraviolet (UV) spectrum, because the band gap of Al_xGa_{1-x}N material covers the entire mid-UV and near-UV spectrum by varying the Al concentration. After the first successful demonstration of UV photodetectors,^{1,2} different types of Al_xGa_{1-x}N based photodetectors such as the Schottky barrier,^{3,4} *p-i-n*,⁵⁻⁷ and metal-semiconductor-metal⁸⁻¹⁰ (MSM) photodetectors have been reported. Those photodetectors had an Al concentration as high as 50% and had a ≥260 nm cutoff wavelength. Since it is difficult to grow high quality and crack-free high Al content material, there are only a few low cutoff wavelength photodetectors reported in the literature.¹¹ The best results were reported by Walker *et al.* where the cutoff wavelength was 235 nm.¹² In this letter, we report the fabrication and characterization of deep UV MSM photodetectors based on Al_{0.75}Ga_{0.25}N epilayers.

Al_{0.75}Ga_{0.25}N epitaxial layers were grown in an Aixtron 200/4 RF-S metal-organic chemical vapor deposition (MOCVD) system on double side polished *c*-plane sapphire substrates. A thin (~50 nm) low temperature AlN nucleation layer and a ~700 nm high temperature AlN buffer layer were used in between the sapphire and the unintentionally doped ~600 nm thick Al_{0.75}Ga_{0.25}N absorption layers. Figure 1 shows the spectral transmission measurement of the epitaxially grown wafer before the fabrication, which was used to determine the Al concentration. The wafer exhibited a 225 nm sharp cutoff, which corresponds to an Al concentration of approximately 75%. The spectrum also has Fabry-Pérot oscillations, implying the high quality of the AlGa_xN layer.

MSM photodiodes were fabricated with a four-step microwave compatible process in a class-100 clean room environment. First 70 Å thick semitransparent interdigitated Au fingers were deposited on an Al_{0.75}Ga_{0.25}N layer. Finger spacing and width varied between 1.5 and 4 μm. Subsequently 100 × 100 and 400 × 400 μm² device mesas along with active areas were defined by CCl₂F₂-based reactive ion etching. The MSM detectors were passivated with an ~120 nm thick Si₃N₄ layer, grown by a plasma enhanced

chemical vapor deposition (PECVD) system. The Si₃N₄ layer was also used as an antireflection layer as well as for protecting the metal fingers. Finally, we deposited 10/400 nm thick Ti/Au interconnect pads.

Current-voltage (*I-V*) characteristics were carried out using a high resistance electrometer with low noise triax cables. The resulting devices exhibited extremely low dark currents and very high breakdown voltages. Figure 2 shows the *I-V* curve of a 4 μm finger width/spacing device. The dark current is below 100 fA up to ±100 V bias voltage, which corresponds to 5.8 × 10⁻¹⁰ A/cm² dark current density under 50 V bias. Even under high bias voltages like 350 V, dark current does not exceed 100 pA. These low dark currents and high breakdown voltages show the high quality of our Al_{0.75}Ga_{0.25}N layers.

Spectral responsivity measurements were performed in the range of 200–400 nm using a Xe lamp, a monochromator, and a calibrated Si photodetector. We recorded the photocurrent using Keithley 6517A electrometer. The resulting responsivity curve as a function of applied bias voltage of a 400 × 400 μm² device with 2 μm/3 μm finger width/spacing is shown in Fig. 3. Devices exhibited a sharp cutoff at 229 nm and a peak photoresponse at 222 nm, which was in good agreement with the transmission measurements. Device responsivity increased with applied voltage and reached 0.53 A/W at 50 V bias voltage under 222 nm UV illumination, which corresponds to a quantum efficiency higher than

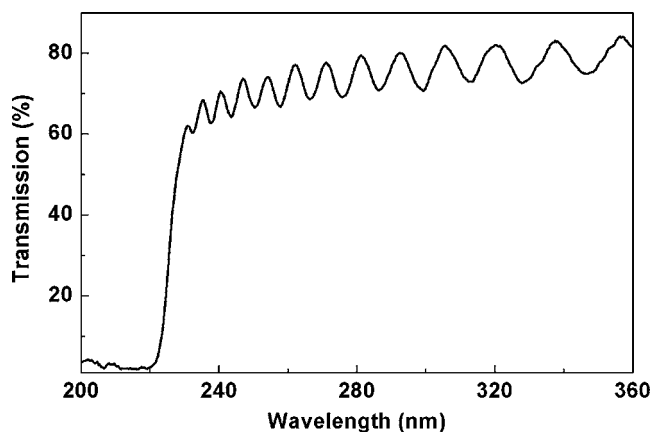


FIG. 1. Spectral transmission measurement of the Al_{0.75}Ga_{0.25}N wafer.

^{a)}Electronic mail: butun@fen.bilkent.edu.tr

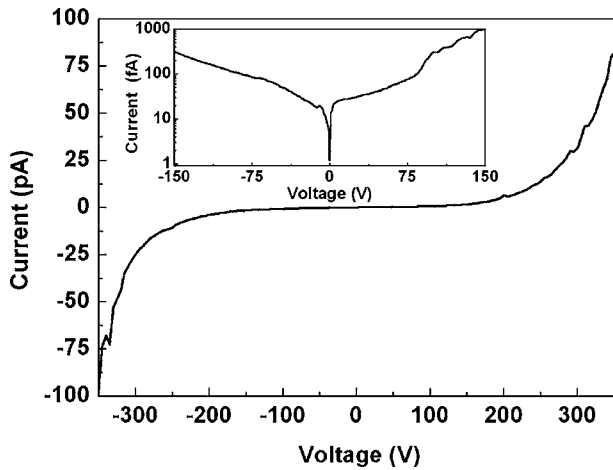


FIG. 2. Dark current measurement of a $100 \times 100 \mu\text{m}^2$ photodetector. Inset: same graph at semilog scale.

250%. This situation can be explained by the photoconductive gain in MSM structures. The inset in Fig. 3 points out that UV-visible (VIS) rejection reached seven orders of magnitude at 20 V bias voltage at 400 nm wavelength. Using the thermally limited detectivity (D^*) formula¹³ $D^* = R_\lambda \sqrt{R_0 A / 4kT}$, where R_λ is device responsivity at 0 V bias, R_0 is the differential resistance, and A is the device area, we find a detectivity of $1.64 \times 10^{12} \text{ cm Hz}^{1/2}/\text{W}$ at 222 nm, which corresponds to a noise equivalent power (NEP) $7.87 \times 10^{-15} \text{ W/Hz}^{1/2}$ at room temperature.

Finally, we performed noise analysis in order to understand the dominant noise mechanism in our detectors. Our setup consists of a fast Fourier transform (FFT) spectrum analyzer, current amplifier, dc voltage source, and a microwave probe station. The noise floor of our setup was $\sim 3 \times 10^{-29} \text{ A}^2/\text{Hz}$ for frequencies higher than 1 kHz and increased at lower frequencies. Most of our detectors exhibited noise densities well below the noise floor. For that reason, we had to investigate devices with relatively high leakage currents. Figure 4 shows the low frequency spectral noise density of a $100 \times 100 \mu\text{m}^2$ device at three different bias voltages. $S_n(f)$ values at 1 Hz are 8.88×10^{-29} , 1.44×10^{-27} , and $8.36 \times 10^{-26} \text{ A}^2/\text{Hz}$ at 0, 25, and 50 V bias voltages,

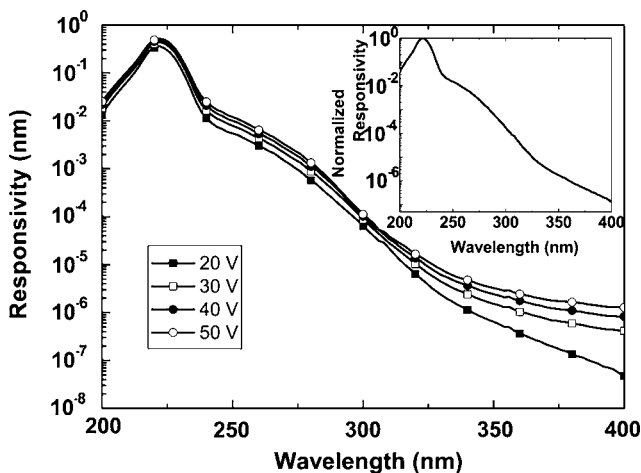


FIG. 3. Spectral responsivity measurements of a $400 \times 400 \mu\text{m}^2$ photodetector. Inset: Normalized responsivity at 20 V bias voltage. (Responsivity at 222 nm is taken as unity.)

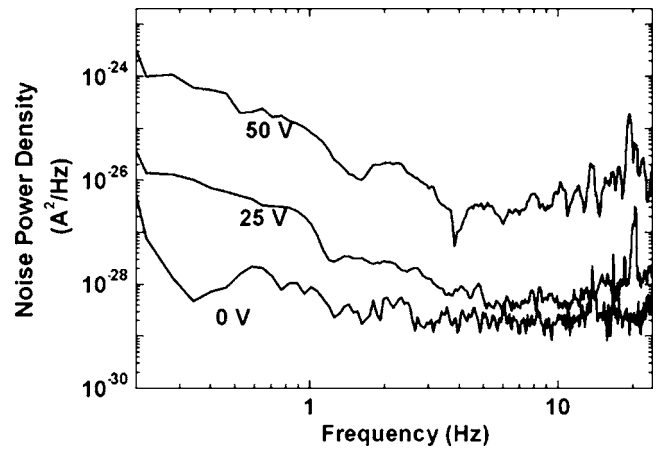


FIG. 4. Spectral noise measurement of a high-leakage $100 \times 100 \mu\text{m}^2$ photodetector with a varying applied bias voltage.

respectively. Noise curves show that $1/f$ (flicker) is the dominant noise mechanism, which is expected for Schottky barrier AlGaIn detectors at low frequencies. Additionally the noise curves obey the relation $S_n = S_0/f^\gamma$ with the fitting parameter γ varying from 1.1 to 1.2. The noise performance and the detectivity performance of our devices show that our MSM photodetectors are suitable for low-noise applications.

In conclusion, we have fabricated and tested deep UV MSM photodetectors on high Al content (75%) AlGaIn templates. The devices have shown a responsivity of 0.53 A/W under 50 V bias and a detectivity of $1.64 \times 10^{12} \text{ cm Hz}^{1/2}/\text{W}$ under 222 nm UV light illumination. The fabricated MSM photodetectors exhibited a low leakage current density of $5.79 \times 10^{-10} \text{ A/cm}^2$ under 50 V bias voltage. They have low noise density and a UV-VIS rejection ratio of seven orders of magnitude, which is a record value for an MSM structure reported in the literature. The cutoff wavelength of 229 nm is the lowest cutoff wavelength reported with AlGaIn based detectors.

¹D. Walker, X. Zhang, P. Kung, A. Saxler, S. Javapour, J. Xu, and M. Razeghi, Appl. Phys. Lett. **68**, 2100 (1996).

²B. W. Lim, Q. C. Chen, J. Y. Yang, and M. Asif Khan, Appl. Phys. Lett. **68**, 3761 (1996).

³A. Osinsky, S. Gangopadhyay, B. W. Lim, M. Z. Anwar, M. A. Khan, D. V. Kuksenkov, and H. Temkin, Appl. Phys. Lett. **72**, 742 (1998).

⁴T. Tut, N. Biyikli, I. Kimukin, T. Kartaloglu, O. Aytur, M. S. Unlu, and E. Ozbay, Solid-State Electron. **49**, 117 (2005).

⁵U. Chowdhury, M. M. Wong, C. J. Collins, B. Yang, J. C. Denyszyn, J. C. Campbell, and D. Dupuis, J. Cryst. Growth **248**, 552 (2003).

⁶C. J. Collins, U. Chowdhury, M. M. Wong, B. Yang, A. L. Beck, R. D. Dupuis, and J. C. Campbell, Appl. Phys. Lett. **80**, 3754 (2002).

⁷M. M. Wong, U. Chowdhury, C. J. Collins, B. Yang, J. C. Denyszyn, K. S. Kim, J. C. Campbell, and R. D. Dupuis, Phys. Status Solidi A **188**, 333 (2001).

⁸T. Li, D. J. H. Lambert, A. L. Beck, C. J. Collins, B. Yang, J. M. M. Wong, U. Chowdhury, R. D. Dupuis, and J. C. Campbell, Electron. Lett. **36**, 1581 (2000).

⁹N. Biyikli, I. Kimukin, T. Kartaloglu, O. Aytur, and E. Ozbay, Phys. Status Solidi C **7**, 2314 (2003).

¹⁰J. Y. Duboz, J. L. Reverchon, D. Adam, B. Damilano, N. Grandjean, F. Semond, and J. Massies, J. Appl. Phys. **92**, 5602 (2002).

¹¹N. Biyikli, I. Kimukin, T. Kartaloglu, O. Aytur, and E. Ozbay, Electron. Lett. **41**, 276 (2005).

¹²D. Walker, V. Kumar, K. Mi, P. Sandvik, P. Kung, X. H. Zhang, and M. Razeghi, Appl. Phys. Lett. **76**, 403 (2000).

¹³S. Donati, *Photodetectors: Devices, Circuits, and Applications* (Prentice Hall, Upper Saddle River, NJ, 2000), p. 43.